

A dielectric anomaly in electrolyte-saturated porous alumina ceramics

F. BROUERS*, A. RAMSAMUGH

*Department of Physics, The University of the West Indies, Mona, Jamaica, West Indies and
Institut de Physique, Université de Liège, Belgium

V. V. DIXIT

Department of Physics, Parks College of St Louis University, USA

In order to understand the relation between the conductivity and the dielectric properties of porous materials and their pore fluid content, we report and discuss dielectric constant measurements of brine-saturated porous alumina ceramics which exhibit a gigantic increase of the low frequency dielectric constant *while the sample remains conducting*. Generalizing a model derived to study the properties of porous sedimentary rocks, where such an effect has been known for more than two decades, we discuss the effect of the pore geometry on the frequency, salinity and porosity variation of the ceramic dielectric constant and conductivity. This can provide a partial explanation of the reported measurements. Such a study provides a new and interesting method to investigate the microgeometry of composite materials and in particular the pore geometry of ceramics.

1. Introduction

During the last few years a number of papers have been devoted to what is generally called the "dielectric anomaly" of rocks. It has been observed that the real part of the dielectric constant $\epsilon'(\omega)$ of brine-saturated rocks at low frequencies (kilohertz range) can be as great as 10^6 . These large values are remarkable considering that the dielectric constant of dry rock and brine are respectively about 10 and 80 [1].

A number of possible explanations have been put forward to explain this interesting phenomenon. In particular, Sen [2] has suggested two possible mechanisms to account for these gigantic values:

(a) A dilute concentration of non-spherical insulating inclusions in a conducting material can yield large values of the dielectric constant even when the sample remains conducting.

(b) Ramified clusters of dead-end pores encased in shells of insulating rocks can give substantial values of ϵ' compatible with a non-zero d.c. conductivity.

These models depend essentially on the microgeometry features of the rocks. The object of this paper is to discuss the applicability of these ideas to porous ceramics.

The employment of ceramics as materials whose porosity and composition can be varied, using well-established preparation methods and thermal treatments, appears to be a convenient way to discuss the theoretical assumptions and conclusions of these models and to contribute to the understanding of the properties of rocks, ceramics and porous materials in general. Such a study provides a new and interesting method to investigate the microgeometry of com-

posite materials and in particular the pore geometry of ceramics. The paper is organized as follows.

In Section 2, we present and discuss brine-saturated porous alumina dielectric constant and conductivity measurements. As in porous sedimentary rocks, large values of ϵ' are observed at low frequencies; the conductivity is frequency-dependent and reminiscent of other types of disordered material. The results vary with salinity and porosity.

In Sections 3 and 4 we consider the two models proposed by Sen. We show that the first is unlikely to be applicable to the ceramics we have studied and that the second model could be considered as a possible explanation provided the model is extended to *non-spherical* dead-end pores.

In Sections 5 and 6 we show that this geometric model can account qualitatively for the variation of the dielectric constant and the electrical conductivity with frequency, porosity and salinity. The model should therefore be considered as a partial explanation of the dielectric and electrical behaviour of electrolyte-saturated porous materials.

We conclude by suggesting more experimental and theoretical investigations.

2. Experimental measurements and data

Al_2O_3 ceramic samples containing < 1% TiO_2 were sintered at temperatures between 1500 and 1600°C for 3 to 18 h. The porosities were determined by measuring their dry weight, wet weight and buoyancy in water. These measurements also give the grain density ρ_g in the range $3.86 \pm 0.02 \text{ g cm}^{-3}$, in approximate agreement with the value for bulk Al_2O_3 . From the small spread in the measured grain density we infer

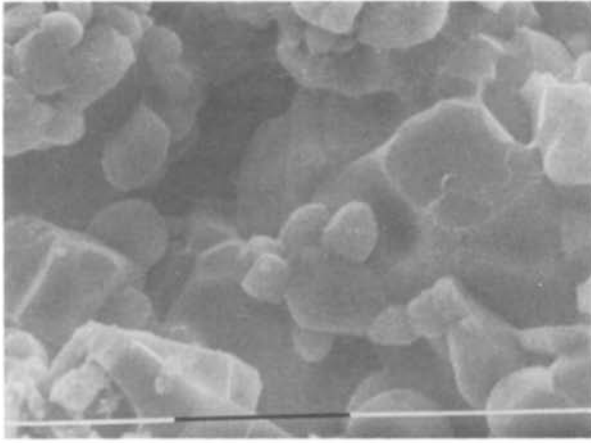


Figure 1 Micrograph of 0.253 porosity Al_2O_3 ceramic. One scale unit is $10\ \mu\text{m}$.

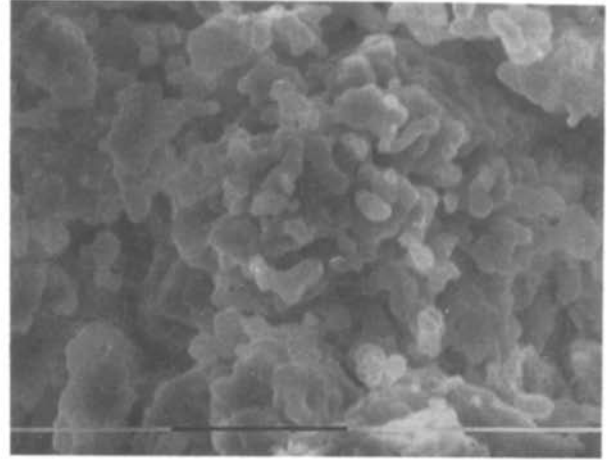


Figure 2 Micrograph of 0.433 porosity Al_2O_3 ceramic. One scale unit is $10\ \mu\text{m}$.

that the occluded volume is essentially very small (less than 2% volume fraction if this exists), i.e. the pore space is almost completely connected and can be fully saturated by the water. Values of porosity and static dielectric constant are given in Table I, and micrographs of two of the samples are shown in Figs 1 and 2.

Al_2O_3 samples in the form of tablets, having the dimensions average diameter = 1.6 cm, average thickness = 0.3 cm, were used. To saturate the samples with brine, they were first placed in a vacuum to remove the air in the pore spaces, and the brine was then let into the evacuated container to fill the pores. Brine solutions of four different conductivities: 0.72, 3.10, 5.61 and $7.29\ \Omega^{-1}\ \text{m}^{-1}$, or alternatively concentration: 0.4, 2.0, 4.0 and 5.6 wt % salinity, respectively, were used.

The brine-saturated Al_2O_3 was sandwiched between metal layers, taking care that the cross-sectional area of the plates was exactly equal to that of the samples, so as to get a fill factor equal to unity. We performed capacitance determinations in the frequency range 10 to 10^6 Hz using a G.R. impedance bridge Type 1650-A, fitted with an external frequency generator. Using this arrangement, the low frequency dielectric constant was also determined for the dry Al_2O_3 samples.

The results of the measurements are reported in Figs 3 to 8. As in sedimentary rocks, large values of ϵ' are observed at low frequencies (Figs 3 to 5). The dielectric constant $\epsilon'(0)$ increases with porosity but is independent of salinity. For frequencies higher than 10^6 Hz ϵ' tends to a value slightly higher than 10, the value for dry ceramic. The cross-over frequency is in the range 10^4 to 10^5 Hz and increases both with salinity and porosity. The values observed are in the range of

those observed for rock dielectric constants [2]. The corresponding conductivities are plotted in Figs 6 to 8. At low and high frequency the conductivity is independent of frequency. Between these two frequencies, which depend on salinity, they exhibit a frequency dependence of $\sigma(\omega) \propto \omega^n$ where n is in the range 0.71 to 0.79. This is compatible with the "universal" pattern of behaviour discussed by Jonscher [3]. We have included the error bars in the upper curve of Figs 3 to 5. These errors, which are large considering the log scale, arise principally from electrode polarization effects, the intrinsic difficulty of measuring the dielectric constant of conducting samples, and possibly the effect of stray impedances. The complex electrode polarization effects arise from the fact that current is carried by electrons in the electrode of the measuring cell, but is carried by ions in the solution. The electron transfer between an ion and the electrode entails a complicated redox reaction which is not properly understood. Stray impedances, both in the measuring cell and in the circuit, can give rise to errors.

In our experiments the following precautions were taken to minimize the above effects: a careful choice of electrodes, the use of a small signal voltage (0.1 V) to limit the current to a minimum, and the use of different sample dimensions (both diameter and length).

3. A model of insulating inclusions

As discussed in Section 1, Sen [2, 4] has proposed two mechanisms to explain the dielectric anomaly in rocks. The first is due to the presence of small plate-like insulating inclusions (clay or other foreign particles) in the conducting rock. The argument is as follows: one starts from the Maxwell-Garnett formula giving the effective dielectric constant ϵ_{MG} of an ellipsoid made of Material B coated by an ellipsoidal shell made of Material A [5-7]:

$$\epsilon_{\text{MG}} = \epsilon_A \frac{(1-g)\epsilon_A + g\epsilon_B + q(1-g)(\epsilon_B - \epsilon_A)}{(1-g)\epsilon_A + g\epsilon_B - qg(\epsilon_B - \epsilon_A)} \quad (1)$$

where ϵ_A and ϵ_B are the dielectric constants of Materials A and B, respectively, q is the volume fraction of

TABLE I Static dielectric constant of porous Al_2O_3 ceramic

Porosity (volume fraction)	Static ϵ
0.433	6.36
0.275	8.14
0.253	8.23
0.193	8.90
0.179	9.27

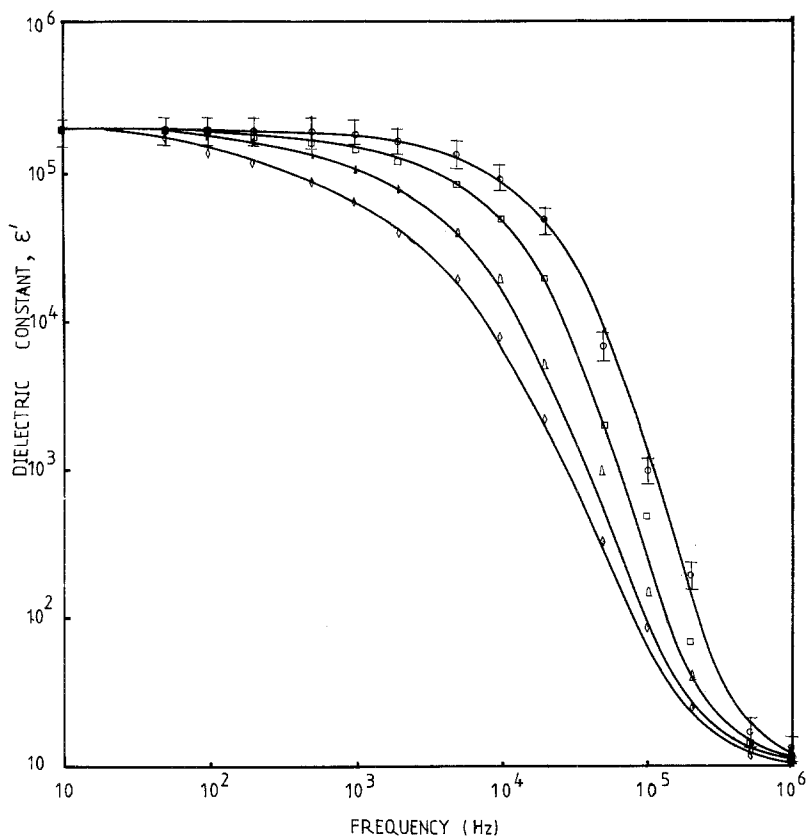


Figure 3 Frequency dependence of the real part of the dielectric constant of brine-saturated alumina ceramics of porosity = 0.179 and four different salinity values. (\diamond) $\sigma_w = 0.72 \Omega^{-1} \text{m}^{-1}$, salinity = 0.4 wt %; (Δ) $3.10 \Omega^{-1} \text{m}^{-1}$, 2.0 wt %; (\square) $5.61 \Omega^{-1} \text{m}^{-1}$, 4.0 wt %; (\circ) $7.29 \Omega^{-1} \text{m}^{-1}$, 5.6 wt %. For dry Al_2O_3 , $\epsilon' = 9.27$.

Material B and g is the depolarization factor in the direction of the field. and

In the present case,

$$\epsilon_A(\omega) = \epsilon'_R + \frac{i\sigma_R(\omega)}{\epsilon_0\omega} \quad (2)$$

$$\epsilon_B(\omega) = \epsilon'_i \quad (3)$$

$$\epsilon_{MG}(\omega) = \epsilon_{Ri}(\omega) = \epsilon'_R + \frac{i\sigma_{Ri}(\omega)}{\epsilon_0(\omega)} \quad (4)$$

where ϵ'_i is the dielectric constant of the inclusions, ϵ'_R and $\sigma_R(\omega)$ are respectively the real part of the dielectric constant and the conductivity of the brine-

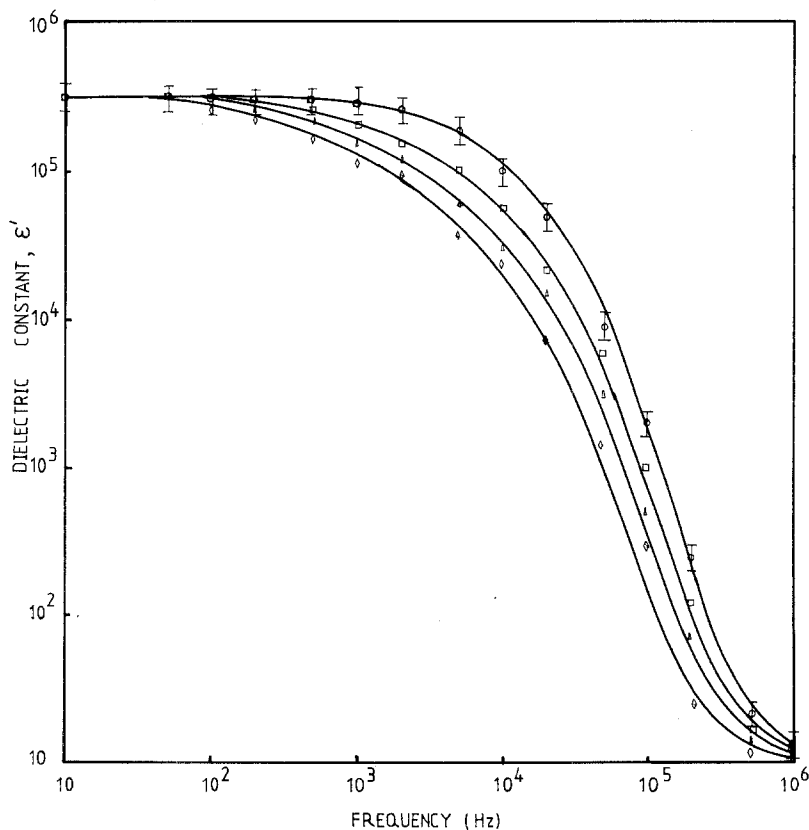


Figure 4 Frequency dependence of the real part of the dielectric constant of brine-saturated alumina ceramics of porosity = 0.253 and four different salinity values. (\diamond) $\sigma_w = 0.72 \Omega^{-1} \text{m}^{-1}$, salinity = 0.4 wt %; (Δ) $3.10 \Omega^{-1} \text{m}^{-1}$, 2.0 wt %; (\square) $5.61 \Omega^{-1} \text{m}^{-1}$, 4.0 wt %; (\circ) $7.29 \Omega^{-1} \text{m}^{-1}$, 5.6 wt %. For dry Al_2O_3 , $\epsilon' = 8.23$.

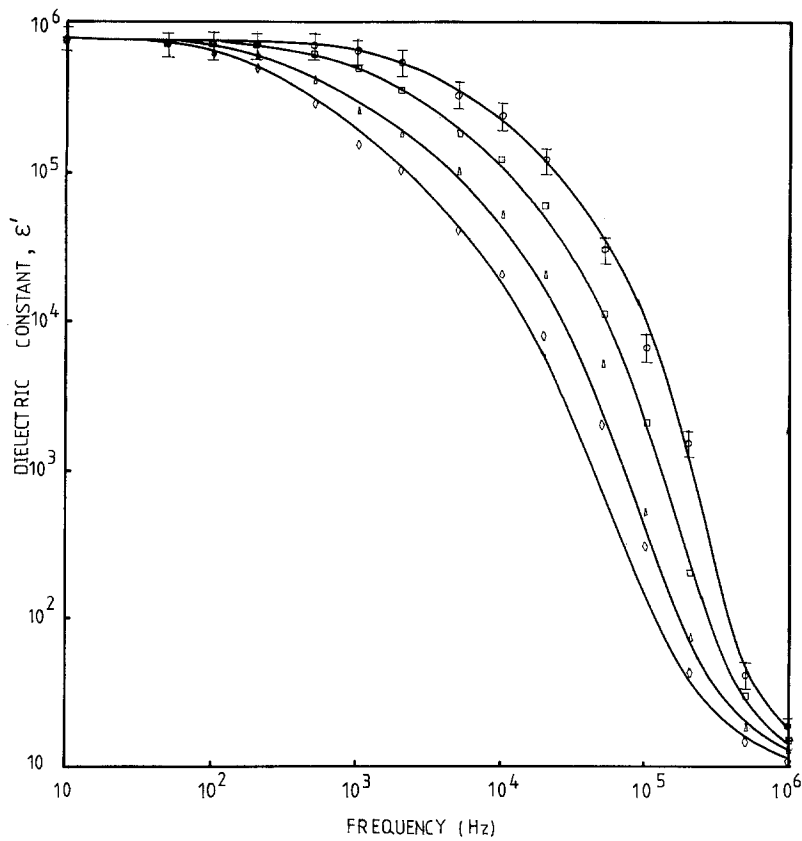


Figure 5 Frequency dependence of the real part of the dielectric constant of brine-saturated alumina ceramics of porosity = 0.433 and four different salinity values. (\diamond) $\sigma_w = 0.72 \Omega^{-1} \text{m}^{-1}$, salinity = 0.4 wt %; (\triangle) $3.10 \Omega^{-1} \text{m}^{-1}$, 2.0 wt %; (\square) $5.61 \Omega^{-1} \text{m}^{-1}$, 4.0 wt %; (\circ) $7.29 \Omega^{-1} \text{m}^{-1}$, 5.6 wt %. For dry Al_2O_3 , $\epsilon' = 6.36$.

saturated rock if there were no inclusions, ϵ'_{Ri} and σ_{Ri} are the corresponding quantities with inclusions and ϵ_0 is the permittivity of a vacuum. The rock d.c. conductivity without and with inclusions is denoted by $\sigma_R(0)$ and $\sigma_{Ri}(0)$, respectively.

The conductivity $\sigma_R(0)$ is related to the porosity ϕ and the water conductivity $\sigma_w(0)$ by the Archie law [8]

$$\sigma_R(0) = a\sigma_w(0)\phi^m \quad (5)$$

The quantity a is close to unity and the exponent m depends on the pore distribution. In our samples m has been found to be equal to 1.92 [8]. The real part of the rock dielectric constant ϵ_R is slightly larger than the dielectric constant of the dry rock ϵ_m (~ 5 to 10).

It can be assumed that $\sigma_R(\omega)$ is frequency-

independent. In this approximation, introducing Equations 2 and 3 into Equation 1, it is easy to show that in the limit $\omega \rightarrow 0$, $q(< 1 - g) \rightarrow 0$

$$\epsilon'_{Ri}(0) = \left(1 - \frac{q}{1 - g}\right) \epsilon'_{Ri} + q \frac{\epsilon'_i}{(1 - g)^2} + 0(q^2) \quad (6)$$

and

$$\sigma_{Ri}(0) = \sigma_R(0) \left(1 - \frac{q}{1 - g}\right) + 0(q^2) \quad (7)$$

when

$$(1 - g)^2 \ll q < 1 - g \quad (8)$$

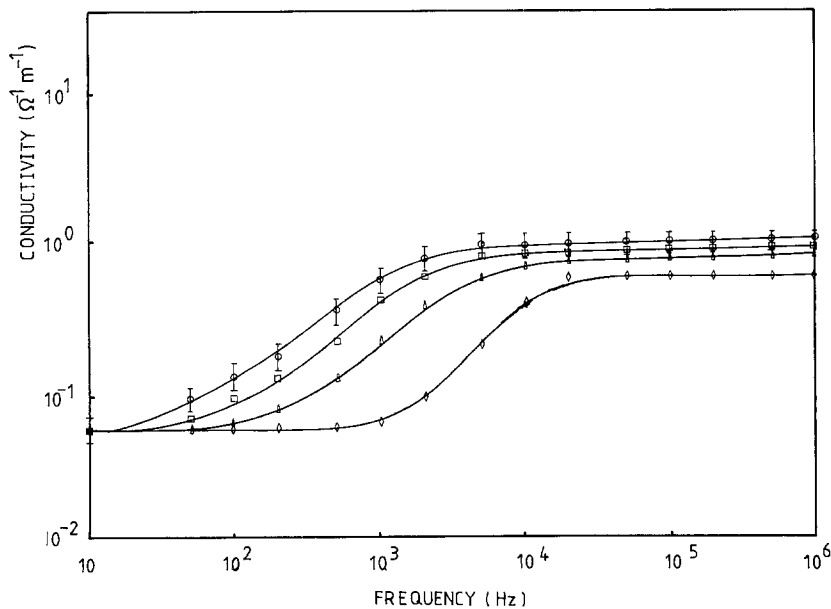


Figure 6 Frequency dependence of the electrical conductivity of brine-saturated alumina ceramics of porosity = 0.179 and four different salinity values. (\diamond) $\sigma_w = 0.72 \Omega^{-1} \text{m}^{-1}$, salinity = 0.4 wt %; (\triangle) $3.10 \Omega^{-1} \text{m}^{-1}$, 2.0 wt %; (\square) $5.61 \Omega^{-1} \text{m}^{-1}$, 4.0 wt %; (\circ) $7.29 \Omega^{-1} \text{m}^{-1}$, 5.6 wt %.

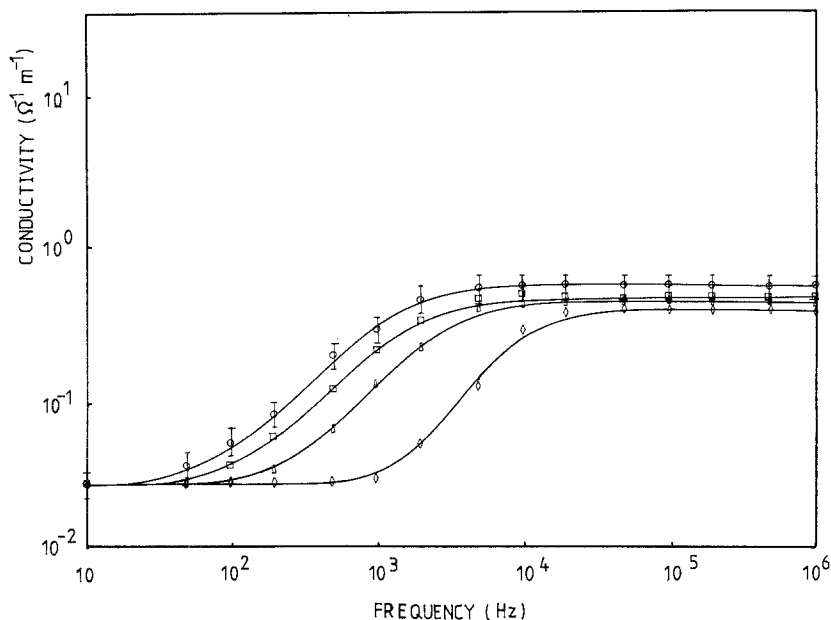


Figure 7 Frequency dependence of the electrical conductivity of brine-saturated alumina ceramics of porosity = 0.253 and four different salinity values. (\diamond) $\sigma_w = 0.72 \Omega^{-1} \text{m}^{-1}$, salinity = 0.4 wt %; (Δ) $3.10 \Omega^{-1} \text{m}^{-1}$, 2.0 wt %; (\square) $5.61 \Omega^{-1} \text{m}^{-1}$, 4.0 wt %; (\circ) $7.29 \Omega^{-1} \text{m}^{-1}$, 5.6 wt %.

one gets a solution where the conductivity is finite together with a high dielectric constant ϵ'_{Ri} . This occurs for very small concentrations of plate-like spheroids with minor axis $a \ll b = c$ when the plate faces are perpendicular to the applied field. In this case,

$$g \approx 1 - \delta \quad \text{with} \quad \delta = \pi a/2b \quad (9)$$

A typical example is $q = 10^{-4}$ and $\delta = 10^{-3}$ for which one gets $\epsilon'_{\text{Ri}} = 10^3$.

A similar result is obtained if one starts from the self-consistent Bruggeman approximation, since both approximations tend to the same expression when $q \rightarrow 0$ [9]. The same effect is obtained in the Sheng approximation, which in the limit $q \rightarrow 0$ reduces to the Maxwell-Garnett approximation.

These results, discussed first by Sen, have a simple physical explanation [2]. The thin plates at low enough frequencies act like capacitors hung parallel to the rest of the rock and hence give a large overall capacitance, i.e. a large dielectric constant.

An examination of the micrographs of Figs 1 and 2 leads to the conclusion that the ceramics do not seem to have such foreign inclusions and that the plate-like grains, observed inside the pore space, do not fulfill the condition of Equation 8. Therefore this first mechanism cannot account for the large values of the dielectric constants that we have measured in these samples.

4. The influence of dead-end pores

We consider now the second mechanism proposed by Sen: a distribution of dead-end pores which yield large values of ϵ' in a non-zero d.c. conductivity material [2].

If the material contains pores or clusters of well interconnected pores which are connected by only a narrow neck to the backbone of pores, this can give relatively large regions of conducting phases surrounded by an insulating coating of grains. These dead-ends can be approximated by conducting water drops encased in an insulating shell. These encased drops are embedded in the conducting host rock.

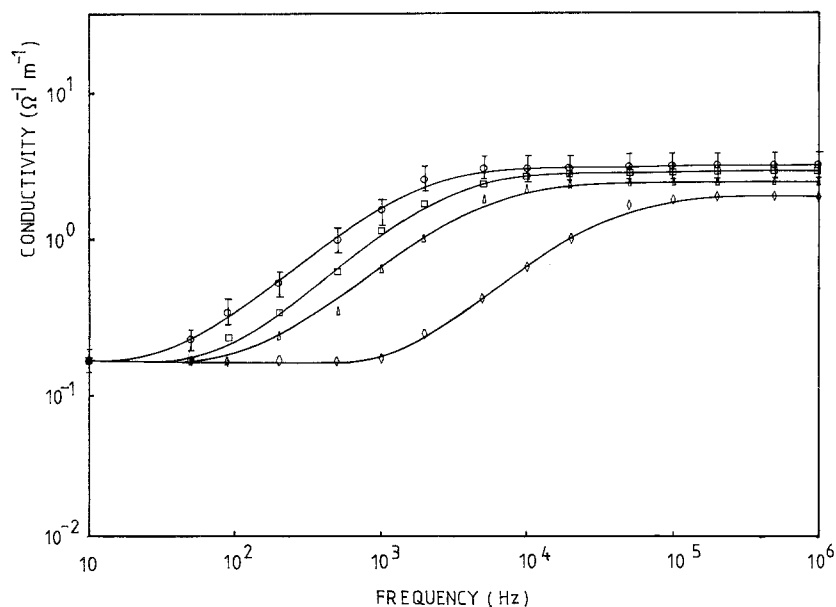


Figure 8 Frequency dependence of the electrical conductivity of brine-saturated alumina ceramics of porosity = 0.433 and four different salinity values. (\diamond) $\sigma_w = 0.72 \Omega^{-1} \text{m}^{-1}$, salinity = 0.4 wt %; (Δ) $3.10 \Omega^{-1} \text{m}^{-1}$, 2.0 wt %; (\square) $5.61 \Omega^{-1} \text{m}^{-1}$, 4.0 wt %; (\circ) $7.29 \Omega^{-1} \text{m}^{-1}$, 5.6 wt %.

Sen [2] has considered the case of spherical droplets. If the thickness of the insulating skin d is much smaller than the radius of the sphere R , the real part of the dielectric constant of the coated sphere is given by

$$\epsilon'_{cs} = \epsilon'_m(R/d) \quad R/d \gg 1 \quad (10)$$

Since these entities are present in small concentrations, the experimental data can be accounted for if $d < 10^{-6} R$, which is obviously unrealistic. For this reason the contribution of these dead-ends was not considered as the main effect by Sen.

The observations of the ceramic micrographs Figs 1 and 2 indicate that the narrow channels which could account for the effect discussed in the dead-end model are far from being spherical. We therefore have to generalize this model to coated ellipsoids. In that case the conditions for obtaining dielectric constants of the order of 10^6 are not as stringent as in Equation 10.

We start from the Maxwell-Garnett formula (Equation 1) where in contrast to the model in Section 3 ϵ_A is an insulator (m) dielectric constant and ϵ_B the dielectric constant of the ellipsoidal coated (water) inclusion (cw), i.e.

$$\epsilon_A(\omega) = \epsilon'_m \quad (11)$$

$$\epsilon_B(\omega) = \epsilon_{cw}(\omega) = \epsilon'_{cw}(\omega) + \frac{i\sigma_{cw}(\omega)}{\omega\epsilon_0} \quad (12)$$

If we consider a random distribution of ellipsoids having the same shape and arbitrary size about fixed orientation with their principal axes parallel to each other, i.e. if we take a fixed scalar depolarization factor g for the entire distribution and calculate a specific component of the dielectric tensor, we obtain

$$\epsilon_{ce} = \epsilon'_m = \frac{(1-g)\epsilon'_m + g\epsilon_{cw} + v(1-g)(\epsilon_{cw} - \epsilon'_m)}{(1-g)\epsilon'_m + g\epsilon_{cw} - vg(\epsilon_{cw} - \epsilon'_m)} \quad (13)$$

where v is the volume fraction of water in the coated ellipsoid; this should not be confused with the porosity ϕ or the concentration q of insulating inclusions in the model of Section 3.

If we write the coated ellipsoid (ce) dielectric constant in the Debye form

$$\epsilon_{ce}(\omega) = \epsilon'_{ce}(\infty) + \frac{\epsilon'_{ce}(0) - \epsilon'_{ce}(\infty)}{1 - i\omega\tau} \quad (14)$$

we get

$$\epsilon'_{ce}(0) = \epsilon'_m \frac{g + v(1-g)}{g(1-v)} \quad (15)$$

$$\epsilon'_{ce}(\infty) = \epsilon'_m \frac{(1-g)\epsilon'_m + g\epsilon'_{cw} + v(1-g)(\epsilon'_{cw} - \epsilon'_m)}{(1-g)\epsilon'_m + g\epsilon'_{cw} - vg(\epsilon'_{cw} - \epsilon'_m)} \quad (16)$$

and

$$\tau^{-1} = \frac{\sigma_{cw}}{\epsilon_0} \frac{g(1-v)}{(1-g)\epsilon'_m + g\epsilon'_{cw} - vg(\epsilon'_{cw} - \epsilon'_m)} \quad (17)$$

If $g = 1/3$, one recovers Sen's expressions for a coated sphere [2]. In particular

$$\epsilon'_{cs}(0) = \epsilon'_m \frac{1 + 2v}{1 - v} \quad (18)$$

In the limit $v \rightarrow 1$, the static dielectric constant $\epsilon'_{ce}(0)$ becomes very large and we have

$$\epsilon'_{ce}(0) = \epsilon'_m \frac{v}{g(1-v)} \quad (19)$$

$$\epsilon'_{ce}(\infty) = \epsilon'_{cw} \quad \text{for any } g$$

$$\tau^{-1} = \frac{\sigma_{cw}}{\epsilon_0} \frac{g(1-v)}{\epsilon'_m} \quad (20)$$

$$\sigma_{ce}(0) = 0 \quad \sigma_{ce}(\infty) = \sigma_{cw}$$

If we compare Equation 19 with Equation 18, we can see that the extra factor $1/g$ can increase considerably the value of the dielectric constant. In the limit $v \rightarrow 1$ and $g \rightarrow 0$ which yields the high dielectric constant values, one has

$$\epsilon'_{ce}(0) \approx \epsilon'_m \frac{1}{g(1-v)} \quad (21)$$

and

$$\tau^{-1}_{v \rightarrow 1, g \rightarrow 0} = \frac{\sigma_{cw}}{\epsilon_0} \frac{g(1-v)}{\epsilon'_m} \approx 10^{11} \sigma_{cw} \frac{g(1-v)}{\epsilon'_m} \text{ sec}^{-1} \quad (22)$$

where σ_{cw} is measured in $\Omega^{-1} \text{ m}^{-1}$. This happens for flat disks with their faces parallel to the applied field or for needles with their axes parallel to the field; in these cases g tends to zero.

For prolate spheroids ($a \gg b = c$) we have

$$g = \left[\ln \left(\frac{2a}{b} \right) - 1 \right] \left(\frac{b}{a} \right)^2 \quad (23)$$

which tends to zero as $a/b \rightarrow \infty$.

If the concentration of these insulating coated ellipsoids is x , the dielectric constant of the medium can be calculated using once more the Maxwell-Garnett formula (Equation 1) with $\epsilon_B = \epsilon_{ce}$ and the rock dielectric constant

$$\epsilon_A(\omega) = \epsilon'_R + \frac{i\sigma_R(0)}{\epsilon_0\omega} \quad (24)$$

In the limit $\omega \rightarrow 0$ and $\omega \rightarrow \infty$ one gets the following expressions:

$$\begin{aligned} \bar{\epsilon}'(0) &= \epsilon'_R - \left(\frac{x}{1-g} \right) \epsilon'_R \\ &+ \left(\frac{x}{(1-g)^2} \right) \epsilon'_{ce} + 0(x^2) \end{aligned} \quad (25)$$

$$\bar{\epsilon}'(\infty) = \epsilon'_R \left(1 + x \frac{[\epsilon'_{ce}(\infty) - \epsilon'_R]}{(1-g)\epsilon'_R + g\epsilon'_{ce}(\infty)} \right) \quad (26)$$

$$\bar{\sigma}(0) = \left(1 - \frac{x}{(1-g)} \right) \sigma_R \quad (27)$$

$$\bar{\sigma}_{g \rightarrow 0}(\infty) = (1-x)\sigma_R + x\sigma_{ce}(\infty) + 0(x^2) \quad (28)$$

$$\bar{\sigma}_{g \rightarrow 1}(\infty) = \sigma_R \left(1 + x - 2x \frac{\epsilon'_R}{\epsilon'_{ce}(\infty)} + x \frac{\epsilon'^2_R \sigma_{ce}(\infty)}{\epsilon'_{ce}(\infty)^2 \sigma_R} \right) \quad (29)$$

In the limit $v \rightarrow 1$,

$$\epsilon'_{ce}(\infty) = \epsilon'_{cw} \quad \text{and} \quad \sigma_{ce}(\infty) = \sigma_{cw} \quad (30)$$

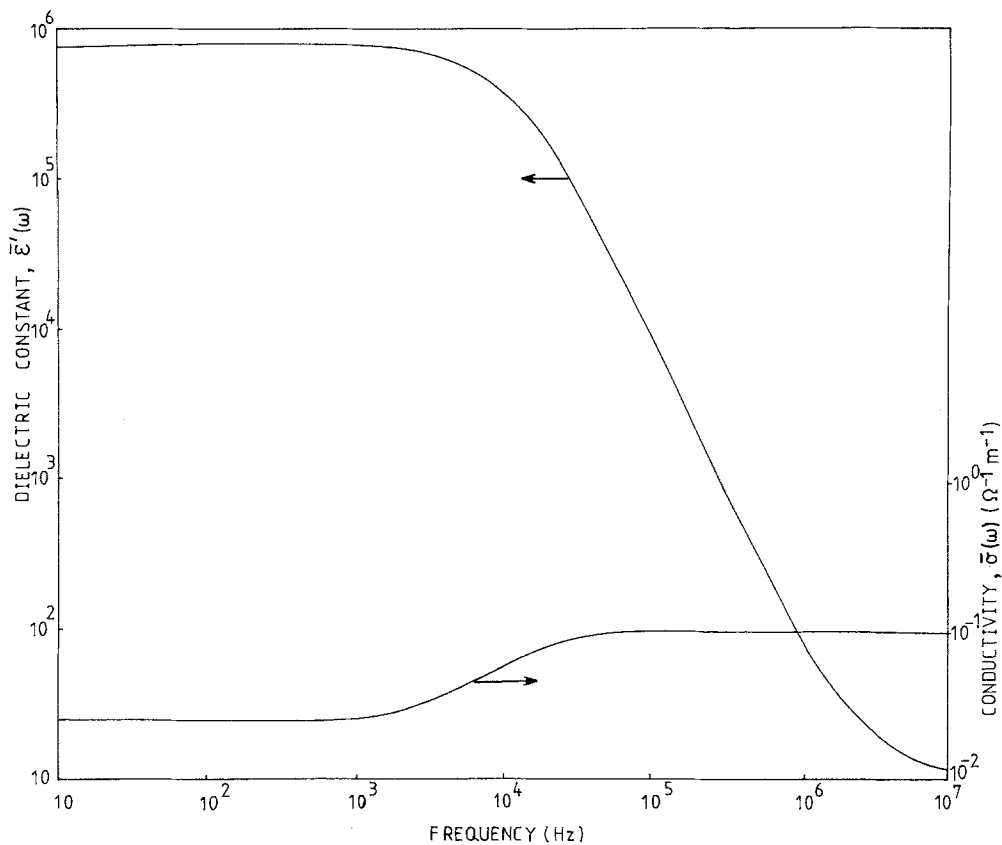


Figure 9 Frequency dependence of the real part of the dielectric conductivity and of the electrical conductivity of an electrolyte-saturated porous material. $x_1 = x_2 = 0.01$, $g_1 = 10^{-4}$, $g_2 = 0.99$, $\nu = 0.999$, $\sigma_{cw} = 6 \Omega^{-1} \text{m}^{-1}$, $\sigma_R = 0.05 \Omega^{-1} \text{m}^{-1}$.

Equation 25 is identical to Equation 6. It must be emphasized, however, that the nature of the insulating inclusions is totally different. In the first model (Section 3) they were foreign particles. Here they are water pockets encased in the insulating Al_2O_3 and are a feature of the ceramic microstructure. The geometric effect described in Section 3 plays a role here too, and therefore coated spheroids with $g \rightarrow 1$ and such that $(1 - g)^2 \ll x < (1 - g)$ can also give a very large contribution to the dielectric constant. In the limit $\nu \rightarrow 1$ this effect is larger than in the first model.

The two effects have to be considered together. If one considers two types of ellipsoids: a concentration x_1 of prolate spheroids ($g \rightarrow 0$) and a concentration x_2 of oblate spheroids ($g \rightarrow 1$) the Maxwell-Garnett approximation (Equation 1) can be generalized and reads

$$\varepsilon_{\text{MG}} = \varepsilon_A \frac{1 + (1 - g_1)x_1\alpha_1 + (1 - g_2)x_2\alpha_2}{1 - g_1x_1\alpha_1 - g_2x_2\alpha_2} \quad (31)$$

with

$$\alpha_i = \frac{\varepsilon_B - \varepsilon_A}{\varepsilon_A + g_i(\varepsilon_B - \varepsilon_A)}; \alpha_i = 1, 2$$

In fact, in porous ceramics there is a distribution of values of g because there is a distribution of aspect ratio and therefore one has to average over ellipsoid orientations and depolarization factors g .

5. Interpretation of experimental data

It is possible to account qualitatively for the experimental data (Figs 3 to 8) as follows:

1. Due to the low concentration x of highly polarized drops, $\varepsilon'_{\text{ce}}(0)$ must be at least of the order 10^6 to 10^7

for prolate spheroids or 10^2 to 10^4 for oblate spheroids. For instance, for $x_1 = x_2 = 0.01$, $g = 10^{-4}$ and 0.99 , respectively, and $1 - \nu = 10^{-2}$.

2. The curves of Figs 3 to 5 obey the limits of Equations 25 and 26.

3. For a given porosity, $\varepsilon'_{\text{ce}}(0)$ and $\bar{\varepsilon}'(0)$ are independent of salinity. The salinity dependence of τ^{-1} arises from the factor σ_{cw} . A decrease of σ_{cw} by an order of magnitude leads to a decrease of τ^{-1} by the same factor.

4. The variation of $\bar{\varepsilon}'(0)$ and τ^{-1} with porosity can be accounted for by Equations 22 to 25. The increase of $\bar{\varepsilon}'(0)$ with porosity is the consequence of an increase of the concentration x with porosity, while the increase of τ^{-1} is the result of an increase of σ_{cw} with porosity.

5. The conductivity increases with frequency as indicated by Equations 25 to 29.

6. At low frequencies $\bar{\sigma}(\omega)$ increases with porosity following the increase of σ_R .

7. The high frequency conductivity $\bar{\sigma}(\infty)$ (Equations 28 and 29) increases with porosity and salinity as σ_{cw} increases with salinity and porosity.

6. Numerical examples

We have performed some numerical calculations to evaluate the results of this geometric effect by considering two types of coated spheroids and using Equation 31 using the following parameters: $x_1 = x_2 = 0.01$, $g_1 = 10^{-4}$, $g_2 = 0.99$ and $\nu = 0.999$, and values of σ_R and σ_{cw} in the range of the experimental values ($\sigma_R = 0.05$ and $\sigma_{cw} = 6 (\Omega^{-1} \text{m}^{-1})$). The dielectric constant of ceramic and saline water are $\varepsilon'_m = 10$ and $\varepsilon'_{\text{cw}} = 80$, respectively. The results are shown in Fig. 9.

7. Conclusions

We have measured the frequency variation of the low frequency dielectric constant and electrical conductivity of brine-saturated alumina ceramics as well as their dependence on salinity and porosity.

We have performed this study in order to obtain information on the nature and distribution of pores and grains and the relation between the dielectric constant, transport properties and microgeometry of composite materials. The employment of ceramics as materials whose porosity can be varied and modified by using various preparation and thermal methods appears to be a convenient way to test proposed theoretical models and to improve our knowledge of the dielectric, electrical and optical properties of this family of disordered systems.

The calculations we have presented demonstrate that the geometry of dead-ends and microchannels must be one of the important factors to be considered to explain the huge values of the dielectric constant as well as the frequency variation of the electrical conductivity.

To make a quantitative theory of these properties, more data are needed and proper averaging procedures have to be devised to account for a variety of possible local microgeometries. The theory should also be extended to deal with mixtures of "com-

ponents" having dielectric constants as different as 10 and 10^6 . In this case the dipolar approximation on which the Maxwell-Garnett approximation is based would be obviously questionable.

Acknowledgements

We would like to thank Dr Duvigneaud of the Laboratoire de Chimie Industrielle, Université Libre de Bruxelles, who prepared the samples.

References

1. J. H. SCOTT, R. D. CAROLL and D. R. CUNNINGHAM, *J. Geophys. Res.* **72** (1967) 5101.
2. P. N. SEN, *Geophysics* **46** (1981) 1714.
3. A. K. JONSCHER, *Nature* **267** (1977) 673.
4. P. N. SEN, *Appl. Phys. Lett.* **39** (1981) 667.
5. J. C. M. GARNETT, *Phil. Trans. R. Soc.* **203** (1904) 385.
6. *Idem, ibid.* **205** (1906) 237.
7. G. A. NIKLASSON and C. G. GRANQUIST, *J. Appl. Phys.* **55** (1984) 3382.
8. G. E. ARCHIE, *AIME Trans* **146** (1942) 54.
9. F. BROUERS and A. RAMSAMUGH, *Solid State Commun.* **60** (1986) 951.
10. BRUGGEMAN, *Ann. Phys. (Liepzig)* **24** (1935) 636.
11. F. BROUERS, *J. Phys. C. Solid State Phys.* **19** (1986) 7183.

Received 15 July 1986

and accepted 15 January 1987